A comparative study of predicting individual thermal sensation and satisfaction using wrist-worn temperature sensor, thermal camera and ambient temperature sensor

Ashrant Aryal, Burcin Becerik-Gerber

Sonny Astani Dept. of Civil and Environmental Engineering, Viterbi School of Engineering, Univ. of Southern California, KAP 217, 3620 South Vermont Ave., Los Angeles, CA 90089-2531, USA

Abstract

Recent advancements in Internet of Things and Machine Learning have opened the possibility of deploying sensors at a large scale to monitor the environment and to model and predict thermal comfort at an individual level. There has been a growing interest to use physiological information obtained from wearable devices or thermal imaging to improve individual thermal comfort prediction. In this study, we compared the accuracies of using environmental sensing with an air temperature sensor, physiological sensing with a wrist-worn device to monitor wrist skin temperature or thermal camera to monitor facial skin temperatures for predicting individual thermal sensation and satisfaction. The experiment was conducted in a controlled environment without any radiant heat sources or local comfort devices; solely the air temperature was changed. For the conditions studied, our results indicate that using data from an environmental sensor for predicting thermal comfort results in a higher accuracy compared to using physiological sensors (either wearable device or thermal camera) alone. Combining data from both environmental and physiological sensors leads to about 3% to 4% higher accuracy than using environmental sensors only. Slight improvement in accuracy from the physiological sensors might not be sufficient to justify the privacy concerns and additional costs of using physiological sensors at a large scale for predicting thermal comfort in environments without radiant heat sources or local comfort devices. Future studies under different environmental conditions with a larger population are needed to better understand the tradeoffs between different sensing methods for predicting thermal comfort at an individual level.

Keywords: Thermal comfort models; Physiological measurements; Infrared thermography; Personalized comfort; Skin temperature

1 Introduction

Ensuring satisfactory indoor environments is the primary goal of Heating, Ventilation and Air Conditioning (HVAC) systems. However, current practice of operating HVAC systems using a "one size fits all" approach fails to satisfy most of the occupants in existing buildings [1]. Current standards such as ASHRAE 55 [2] and ISO 7730 [3] rely on the Predicted Mean Vote and Predicted Percent Dissatisfied (PMV/PPD) model for air conditioned buildings and the adaptive comfort model for naturally ventilated buildings to establish acceptable indoor thermal conditions. Although the standards specify the requirement of satisfying at least 80% of the occupants in a building, a large scale study that surveyed occupants in commercial buildings across North America showed that only 38% of the occupants were satisfied with their indoor thermal environment [1]. HVAC systems are responsible for about 50% of building energy consumption in the U.S. and European countries [4]. Despite their large energy consumption share, HVAC systems fail to meet the primary purpose of ensuring satisfactory indoor environments for building occupants. The low rate of occupant satisfaction arises due to the individual differences in thermal preferences among occupants

and the inability of current HVAC systems to meet individual preferences due to lack of personalized conditioning and control [1,5].

Thermal comfort is defined in ASHRAE 55 as the condition of mind that expresses satisfaction with the thermal environment and is assessed by subjective evaluation [2]. The PMV and adaptive comfort models are based on averaged responses from a large population and are unable to accommodate the differences in estimating thermal comfort responses of individuals. A recent study using the ASHRAE Global Thermal Comfort Database II, the largest database of thermal comfort observations to date, demonstrated that the PMV model was only 34% accurate in predicting actual thermal sensations of building occupants [6]. In order to overcome the limitations of the PMV and adaptive comfort models, several researchers developed methods to model and predict thermal sensation, preference or satisfaction at an individual level [7–12]. Such models typically rely on different sensors to monitor environmental parameters, such as air temperature, humidity, mean radiant temperature or physiological parameters, such as skin temperature to build individual comfort models using different Machine Learning (ML) techniques. The goal of such methods is to use individual comfort predictions from the models to control HVAC systems or other Personal Comfort Systems (PCS) to improve occupant comfort and satisfaction with indoor thermal environments [7].

With the recent advancements in Internet of Things (IoT), collecting physiological data using different wearable and/or non-wearable devices is becoming prevalent. This has led to an increase in studies focused on predicting thermal sensations from physiological parameters, such as heart rate, blood pressure, skin temperature from different locations on human body, such as wrists, face, back, legs monitored using wearable devices [13–17]. Recent studies have also considered monitoring skin temperature using non-intrusive methods, such as infrared thermal imaging [11,18–20]. Using skin temperature to predict thermal comfort typically results in higher accuracy of thermal comfort prediction compared to other methods, however, such devices are more expensive compared to environmental sensors. Moreover, privacy concerns surrounding the use of physiological data may limit user acceptability. In this study, we evaluate the accuracy tradeoffs between using a wrist-worn wearable device, a thermal camera or an ambient air temperature sensor to predict individual thermal comfort.

The rest of the paper is organized as follows. In section 2, we review the literature to summarize the progress towards personalized thermal comfort prediction and control. We discuss our methodology in section 3, followed by the results presented in section 4. We discuss the limitations and practical implications of our results in section 5 and conclude the paper in section 6.

2 Literature Review

Early research on modeling of thermal comfort involves the seminal work of P.O. Fanger in 1970 when he developed the PMV/PPD models based on heat balance of the human body [21]. The model relies on measurement of four environmental parameters: air temperature, radiant temperature, air speed and relative humidity; and two personal parameters: clothing insulation and metabolic activity [21]. The PMV/PPD model is adopted by international guidelines, such as ASHRAE 55 [2] and ISO 7730 [3] and is still the official model to evaluate thermal comfort in buildings. The PMV/PPD model ignores the behavioral, psychological and physiological (other than metabolic rate) factors that influence thermal comfort. A major development in the field of thermal comfort was the introduction of the adaptive model of comfort in 1998 by de Dear and Brager [22]. The adaptive model considers different physiological (acclimatization), psychological (changing thermal expectations) and behavioral (e.g., operating windows, fans) opportunities that occupants have in order to adapt themselves to maintain thermal comfort. ASHRAE 55 includes the

adaptive model [22] as a method to determine acceptable thermal conditions for naturally ventilated buildings. Further details of the PMV/PPD and adaptive models can be found in [21–25].

The major limitation of both the PMV/PPD and adaptive models is the "one size fits all" approach because they were developed based on the average response from a large population. Due to the inability of these methods to accommodate for individual differences in thermal comfort requirements, researchers have recently focused their efforts on modeling thermal comfort at an individual level [7]. Earlier efforts in personal comfort models relied primarily on the sensor data from monitoring environmental parameters, such as air temperature and humidity, and utilized different ML methods to map sensor measurements to comfort feedback collected from the participants. For example, Feldmeier and Paradiso utilized a wrist worn device to monitor air temperature and humidity around the occupant and used a linear discriminant method to separate hot and cold sensations [26]. Daum and Haldi utilized air temperature to model personal comfort profiles using logistic regression [8]. Zhao et. al. used recursive least square estimation to tune parameters of a nonlinear heat balance equation for each individual to build personalized models [27]. Other approaches include the use of fuzzy-logic models [28], Bayesian network [9], C-Support Vector Classification [29] and random forest classification [30] for predicting thermal comfort at an individual level.

Human body maintains its core temperature within a narrow range around 36°C to 38°C using the natural process of thermoregulation [31]. The primary mechanisms of thermoregulation involve vasodilation, vasoconstriction, sweating and shivering. Cold environments can result in shivering to increase heat generation and hot environments can result in sweating, which increases heat loss via sweat evaporation. In cold environments, the skin blood vessels constrict (vasoconstriction), which reduces skin blood flow resulting in decreased skin temperature and reduced heat loss. In hot environments, skin blood vessels dilate (vasodilation), which increases skin blood flow resulting in higher skin temperature and increased heat loss [31]. Extensive climate chamber studies conducted at the Center for Built Environment at Berkeley provide an insight into how skin temperatures in different body parts change under different thermal environments and how the changes relate to local and whole body thermal sensations [32–37]. In uniform neutral environments, the trunk feels close to neutral, the face, hand and arms feel warmer than neutral and the foot feels cooler than neutral, which is also consistent with the skin temperature distribution of the body [34]. The overall thermal sensation during cool and cold uniform environments is strongly affected by the sensations in the extremities (arm, hand, leg, foot), and the overall thermal sensation in warm and hot environments is strongly influenced by the thermal sensation of the face and head region [32]. Under non uniform conditions, the overall thermal sensation closely follows the sensation in two most uncomfortable body parts [32,37].

Other climate chamber studies outside of Berkeley have also studied physiological responses under different environmental conditions. Yao et al. observed that the mean skin temperature decreases gradually when going from hot to cold sensations and the maximum difference in local skin temperature increases gradually when going from hot to cold sensations [38]. Sakoi et al. observed that in non-uniform thermal environments using radiant heaters, the local heat discomfort in the head region was dependent on the local skin temperature and local heat loss, and local cold discomfort in the foot area was related to local skin temperature [39]. Choi et. al. monitored skin temperatures from 16 different body sites and found that skin temperatures from the forehead, arm, back and wrist showed significant correlation with thermal sensations, with wrist being the most correlated site [15]. In another study, Choi et. al. found that skin temperatures from the forehead and back of the wrist were highly correlated with thermal satisfaction [13]. Xiong et. al. studied changes in skin temperatures from seven different sites on a body under transient conditions and found that back, arm and leg were most related to changes in overall thermal sensation [14]. Although the

previous studies were performed in climate chambers, they help to improve our understanding of how skin temperature could be used to predict thermal sensations. Because skin temperature at different locations change differently under uniform and non-uniform conditions, monitoring skin temperature can provide more insight into thermal sensation and comfort compared to monitoring environmental parameters only. Due to the usefulness of skin temperature and advancements in small and convenient sensors, there has been an increase in studies that utilized physiological measurements for predicting thermal comfort in recent years.

One of the practical methods of monitoring changes in skin temperature and other physiological data is to use wearable devices; several studies have explored the feasibility of using such devices. Chaudhuri et. al. monitored skin temperature from the back of the hand under cold to neutral conditions, and utilized Support Vector Machine (SVM) and Extreme Learning Machine (ELM) classifiers and achieved 87% accuracy in predicting thermal sensations [40]. In another study, Chaudhuri et. al. achieved an accuracy of about 93% by monitoring hand skin temperature, skin conductance, pulse rate, blood oxygen saturation and blood pressure and using a random forest classifier to classify comfortable and uncomfortably cold conditions [41]. Liu et. al. achieved the mean accuracy of 75% in predicting thermal preferences using skin temperature and heart rate, and environmental parameters using a random forest classifier [17]. Sim et. al. monitored skin temperatures from the wrist and fingertips and used a linear regression model to achieve a RMSE (root mean square error) of 1.26 on a 9 point thermal sensation scale [42]. Abdallah et. al. used several environmental and physiological parameters as input to Artificial Neural Networks (ANN) to achieve an RMSE of 0.023 on a 7 point thermal sensation scale for four participants in the study [43]. Ghahramani et. al. used infrared temperature sensors mounted on an eyeglass frame to monitor changes in skin temperature from different points on human face and achieved 83% accuracy for detecting uncomfortable conditions using a hidden Markov model [16].

Wearable devices can be considered intrusive and some occupants may not be willing to wear a device consistently. To address this issue, several studies have used non-intrusive techniques based on thermal imaging to extract skin temperatures from different body sites. For example, Pavin et. al. found that temperatures extracted from the forehead region using a thermal camera were well correlated with thermal sensations [18]. Burzo et. al. used manually extracted temperature from thermal images, combined with other physiological measurements to train decision tree classifiers resulting in 74% accuracy in predicting thermal sensations [20]. Ranjan et. al. used images obtained from a thermal camera to manually extract temperatures from different regions of the face and hand. The extracted skin temperatures along with environmental measurements were used to train random forest classifiers to predict thermal preferences, which resulted in an accuracy of around 95% when separate models for heating and cooling conditions were built [44]. Cosma et. al. developed a method to automatically extract temperatures from different body sites using a thermal camera and a Kinect sensor and found that variance of face temperatures correlated with thermal sensations [19]. Li. et. al. found that temperatures extracted from ears, nose and cheeks using a thermal camera were most indicative of thermal comfort and achieved an accuracy of 85% using random forest classifier [11].

In addition to skin temperatures, other physiological parameters, such as electroencephalogram (EEG), heart rate, heart rate variability and other cardiovascular parameters derived from electrocardiogram (ECG) have been investigated and might also reflect changes in thermal comfort [30,38,45,46]. However, changes in skin temperature are used more widely compared to other physiological measurements for thermal comfort assessment because skin temperature is directly affected by the thermoregulation system and can be easily monitored in various body locations. In general, older studies relied on monitoring environmental parameters to model individual thermal comfort, and recent studies relied more on physiological parameters

for modeling thermal comfort. Skin temperature seems to be the most suitable physiological parameter for assessing thermal comfort. From a practical standpoint, either using a wearable device (e.g. smartwatches) to monitor skin temperature from the wrist or using a thermal camera to monitor skin temperatures from the face might be more appropriate compared to other body sites. Since different researchers relied on different methods, there is a lack of a well-accepted approach for sensing and modeling of thermal comfort. Furthermore, the use of different approaches prohibits a direct comparison of different sensing and modeling methods for thermal comfort prediction. In this study, we evaluate the accuracy of predicting thermal sensation and thermal satisfaction that can be obtained by monitoring ambient temperature, skin temperature from the wrist using a wearable device and facial temperatures monitored using an infrared thermal camera. We attempt to answer the question: *"What are the most suitable sensing and machine learning methods for modeling of thermal sensation and satisfaction at an individual level?"*

3 Methodology

The overall methodology used in this study involves a climate-controlled experiment where participants were exposed to different temperatures while different sensors were used to monitor changes in the air temperature and skin temperature while thermal sensation and satisfaction votes were collected from the participants. The collected information was used to train different ML models to predict participant thermal sensation and satisfaction. We describe the methodology in detail in the following subsections.

3.1 Experiment procedure

The data were collected in a research office at the University of Southern California (USC) in Los Angeles during the summer months of June 2018 to August 2018. The climate of the location is classified as warm-summer Mediterranean climate according to the Koppen-Geiger climate classification [47]. The average outdoor temperature during the study period was 26°C with the average high and low outdoor temperatures ranging from 21°C to 31°C, respectively. All of the participants were asked to wear pants and t-shirts during the experiment to keep the clothing levels consistent. The experiment procedure was explained to the participants and informed consent was obtained before starting the experiment. The study was approved by the Institutional Review Board (IRB) at USC. Twenty healthy subjects, 12 males and 8 females, participated in the study. The anthropometric details of the study participants are shown in Table 1.

Table 1: Anthropometric details of study participants

Gender	Count	Age(years)	Height(cm)	Weight(kg)
Male	12	23.9 ± 4.6	178.6 ± 6.8	80.0 ± 13.0
Female	8	29.5 ± 14.8	161.6 ± 7.2	64.5 ± 16.5
Overall	20	26.2 ± 10.1	171.8 ± 10.9	73.8 ± 16.1

Each participant was given an ID number and asked to provide feedback about their thermal sensation and satisfaction using a web interface shown in Figure 1. The ASHRAE 7-point thermal sensation scale was used to collect their thermal sensation, and a 7-point satisfaction scale was used to gather thermal satisfaction every 5 minutes during the study using the interface. Participants were seated during the experiment and were asked to work normally using their laptop.

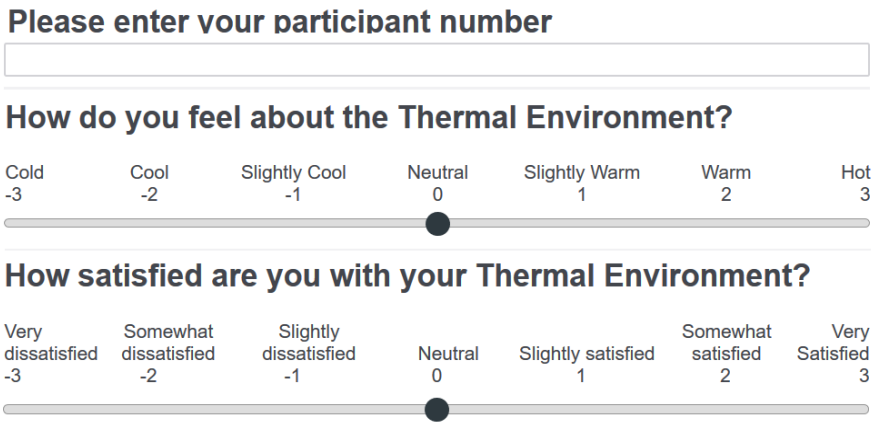

Figure 1: Web interface to collect participants comfort and satisfaction

The experiment was conducted in two separate segments: cold segment and hot segment. The order in which the participants participated in the two segments was randomized to avoid potential bias resulting from thermal expectations. For instance, participants may anticipate feeling cold if they know it is a cold segment. In the cold segment the temperature was gradually decreased from roughly 24°C to 19°C, and in the hot segment the temperature was gradually increased from roughly 22°C to 29°C. The cold segment started at temperatures slightly above typical neutral condition (23 °C), and the hot segment started slightly below typical neutral conditions. This enabled the participants to start at a neutral temperature for both segments and avoid sudden overshoot in thermal sensations when participants moved from a neutral environment outside into the study room. Temperatures outside the range of 19°C to 29°C were not studied as they are unlikely to be experienced in HVAC operated buildings. Each segment lasted between 1 to 1.5 hours and was stopped when the participant voted +3 or -3 for two consecutive times or when 1.5 hours was over. It is important to note that participants were not aware of the early stopping criteria to avoid potential bias due to participants voting +3 or -3 to finish the experiment early, and participants were simply told that the experiment duration was over. The reason behind this approach was to gather data relating to all possible ranges of thermal sensations without causing too much discomfort to the participants and reduce unnecessary harm to the participants, per the IRB approval. There was least 1-hour gap between the segments where the room was adjusted to the new starting point and participants were transferred to another location with a neutral temperature during this period for the participants to re-acclimate to the neutral environment. The room temperature was changed gradually at the rate of roughly 1°C/10 mins to avoid sudden changes in the thermal environment during both segments. The minimum air temperature and its standard deviation for the participants during the experiment was 19.3 ± 1°C. The maximum air temperature and its standard deviation was 28.7 ± 0.6 °C. The average duration of the cold segment was 66.4 ± 9.2 mins and average duration of the hot segment was 68.7 ± 15.1 mins. The temperature change rates during the cold segments was 0.7 ± 0.2 °C/10 mins, and 0.1 ± 0.2 °C/10 mins during the hot segments. During the experiments, 16 participants reported a thermal sensation of either +3 or -3, and 9 participants reported thermal sensation of both +3 and -3.

In addition to the thermal sensation and satisfaction feedback collected directly from the participants, we used different sensors to monitor. There sensors were: (1) ambient air temperature, (2) skin temperature from the wrist using a wearable device and (3) a thermal camera to monitor skin temperature from different regions of the face. Room air temperature was monitored every second using a DHT22 sensor connected to an Arduino Uno placed on the desk roughly 0.5m from the participant. The DHT22 sensor has an accuracy of ±0.5°C and resolution of 0.1°C for temperature measurements. Skin temperature was collected every

second from the wrist using a MLX90614 contact-less infrared temperature sensor placed roughly 1cm from the skin which was fitted on a wristband worn by the participant. The MLX90614 sensor has an accuracy of ±0.5°C and resolution of 0.02°C for temperature measurements and was connected to an Adafruit Feather data logger. A FLIR Lepton thermal imaging camera from Tinkerforge was used to capture thermal images, and a standard web camera was used to capture RGB images of the participants' face every second during the experiment. The cameras were placed roughly 1 meter away from the participants. FLIR Lepton is a low-cost thermal camera which is capable of taking 80×60-pixel thermal images and has an accuracy of ±5°C and a resolution of 0.1°C for temperature measurements. Although higher resolution thermal cameras are available, FLIR Lepton was selected due to its low cost and thus its potential to be deployed at a larger scale. FLIR Lepton was previously validated by Li et. al. [11] against the FLIR T450SC camera which is capable of capturing 320×240 pixel thermal images with an accuracy of ±2°C, and the authors showed that the FLIR Lepton camera was adequate for monitoring changes in skin temperature. The FLIR lepton camera is factory calibrated to provide accurate measurements and automatically performs recalibration when the sensor temperature changes [48], therefore, sensor calibration was not performed in this study. The experiment setup for this study is shown in Figure 2. The wearable device also had a Galvanic Skin Response (GSR) sensor, but measurements from the GSR sensor were not used in this study because the sensor was unreliable.

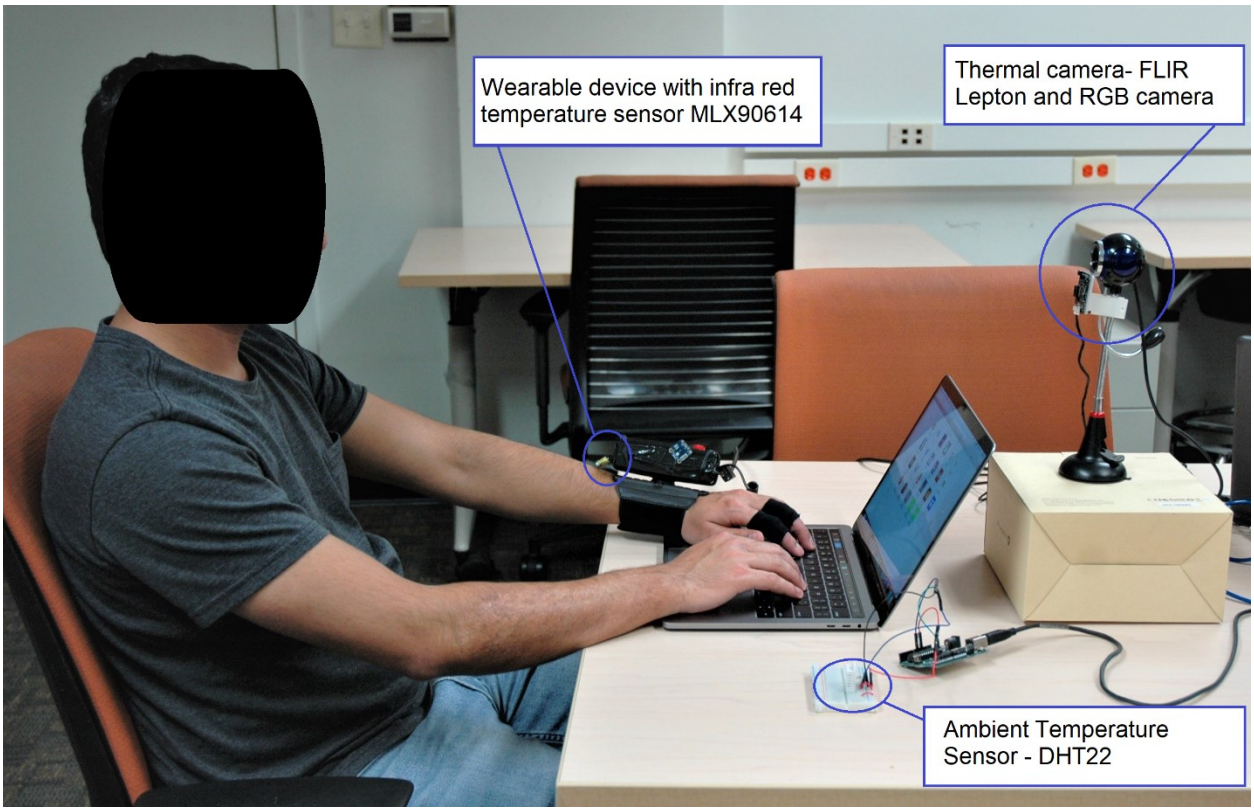

Figure 2: Experiment setup

3.2 Data Analysis

The data analysis consists broadly of three stages: (1) data cleaning and preprocessing, (2) feature extraction, and (3) training and evaluation of different ML algorithms to predict thermal sensation and satisfaction.

3.2.1 Data cleaning and preprocessing

Measurements from the ambient air temperature and wrist skin temperature sensors were first passed through a Hampel filter to remove outliers in data caused due to disturbances in the sensor connections [49]. Then a Savitzky-Golay filter was used to smooth the sensor signals and remove some of the noise in the measurements [50]. The Savitzky-Golay filter is a popular signal smoothing algorithm that fits a low degree polynomial function to sets of adjacent points in a sliding window using least squares method and evaluates the resulting polynomial, which removes some noise from the signal without greatly distorting the sensor signal [50]. The sensor signals before and after the filter process is shown in Figure 3 for a participant in both cold and hot segments.

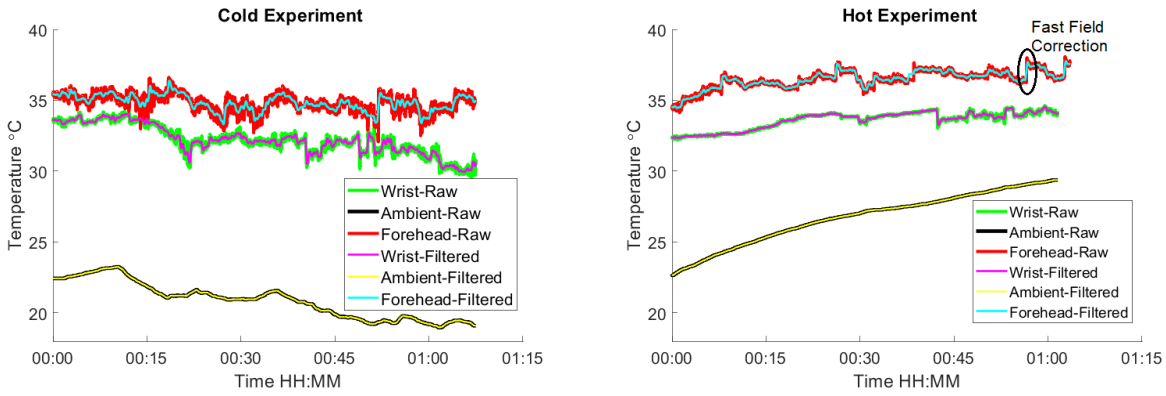

Figure 3: Sensor measurements before and after filtering of a participant's data

In this study, we extracted temperatures from four Region of Interest (ROI) on the face using thermal images: forehead, nose, left cheek and right cheek. These ROIs were selected because previous studies identified them to be important for thermal sensation prediction [11,16,51]. Although studies [11,16] also identified ears to be important, it is not feasible to obtain continuous measurements from the ears because ears can get occluded from the images even with small movements or covered by hair for female participants. Furthermore, the low resolution of the thermal camera makes it difficult to distinguish ears from the face. Thus, temperature measurements from ears were not used in this study.

For extracting temperatures from the face using the thermal camera, first the RGB image was overlaid on the thermal image using a 2-D image transformation. A Facial Landmark detection algorithm developed by Kazemi et. al. [52] was then used to identify different regions of the face, such as eyes, nose, mouth etc. on the RGB image. Using the location of different landmarks, the locations of different ROI were automatically identified in the overlaid RGB image based on their relative locations in reference to the landmarks. Then, the corresponding locations in the thermal image were used to obtain the temperature measurements. Figure 4 shows the thermal image obtained from the thermal camera, the RGB image overlaid on top of the thermal image along with the detected facial landmarks, and the thermal image with identified ROIs of nose, forehead, left cheek and right cheek. Since the resolution of the thermal image obtained from FLIR Lepton camera is not high enough to robustly identify different regions of the face, we utilized the RGB image to first identify different ROIs and then obtained the corresponding temperature measurements from the thermal image. The extracted temperature measurements were then filtered using the Hampel filter and Savitzky-Golay filter similar to other sensor measurements. Figure 3 also shows the measurements from the forehead of one of the participants before and after the filtering process. Measurements from nose, left cheek and right cheek are not shown to make Figure 3 more legible but they follow a similar trend to the forehead temperatures.

It is important to note that the FLIR Lepton camera performs a Flat-Field Correction (FFC) every 3 minutes or when the camera temperature changes by 3°C to correct for the temporal drift, which accumulates over time and can result in degraded image quality [48]. The FFC process recalibrates the camera to improve the image quality but can result in sudden shifts in temperature measurements before and after the FFC process. One such instance of the FFC correction is shown in Figure 3 for illustration. Although this correction results in sudden shifts in temperature, the overall trend is preserved. Furthermore, the filtering process does not remove this artifact since this artifact results from the camera itself.

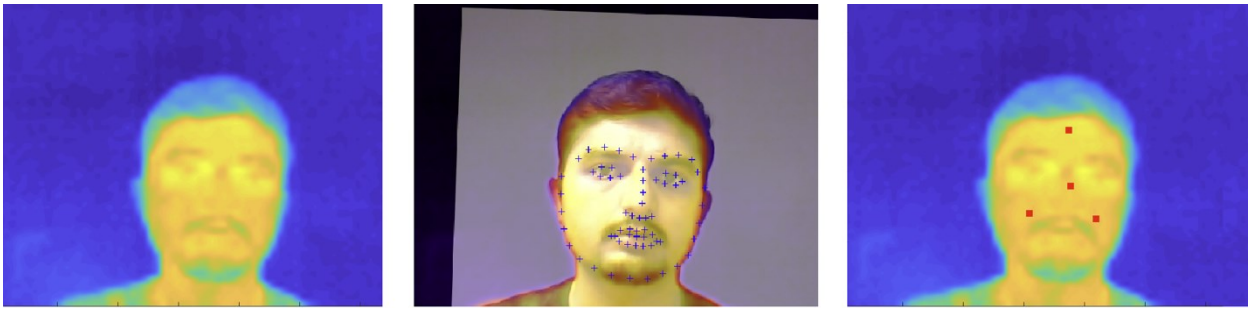

Figure 4: Steps of temperature extraction from different ROIs in thermal images. From left to right: thermal image, landmark detection using RGB image overlaid on thermal image, identified ROIs on thermal image.

3.2.2 Feature extraction

The cleaned sensor measurements were mapped to the corresponding Thermal Sensation Vote (TSV). Figure 5 shows the cleaned measurements for ambient temperature, wrist skin temperature and forehead skin temperature along with the corresponding TSVs for one of the participants. Measurements from other ROIs in the face are similar to the measurements from the forehead and are not shown in Figure 5 to make the figure more legible. Several features were extracted from each of the six temperature data streams: ambient, wrist, forehead, nose, right cheek and left cheek temperatures for training different ML algorithms. For each data stream, 18 features were extracted for each five-minute window before every recorded TSV. The features relate to four different categories: 1) Direct value of measurements, 2) Derivative of the measurements, 3) Shape of data streams, and 4) Recent measurements. The features related to direct value of the measurements include the minimum, maximum, average, standard deviation and median of the measurements in the five-minute window. Features related to the derivative include the minimum, maximum, average, standard deviation and median of the first derivative of the data stream. The features to capture the shapes of the data streams include the coefficients obtained by fitting a first degree (2 coefficients) and second degree (3 coefficients) polynomials to the measurements in the five-minute window. Features to capture recent measurements include the most recent measurement value, average value of last 10 seconds, and average of the first derivative for the last 10 seconds. The goal of extracting these features is to capture the overall values, trends and patterns of changes in the data streams. Features relating to the value of measurements and the derivative of measurements have also been used in previous studies [11,41] for predicting thermal comfort. Additional features to capture the shape of the data streams were added in this study because the features based on direct value and derivative of measurements do not capture how the data stream changes over time. A total of 108 features were extracted from the sensor data, 18 from air temperature, 18 from wrist temperature, and 72 (18×4) from the 4 ROIs from the thermal camera, for each corresponding TSV.

Prior to training the classification algorithms, feature selection was performed to remove the features that were not useful for the classification problem. Removing unnecessary and redundant features can improve

the performance of classification algorithms both in terms of speed and generalization performance. A Neighborhood Component based feature selection was used to eliminate unnecessary features prior to model training [53]. The Neighborhood Component based feature selection is a supervised feature selection approach, which learns the weights for each feature by maximizing the expected leave-one-out classification accuracy with a regularization term. The feature selection process also gives insight into which features are the most useful in predicting thermal comfort and satisfaction.

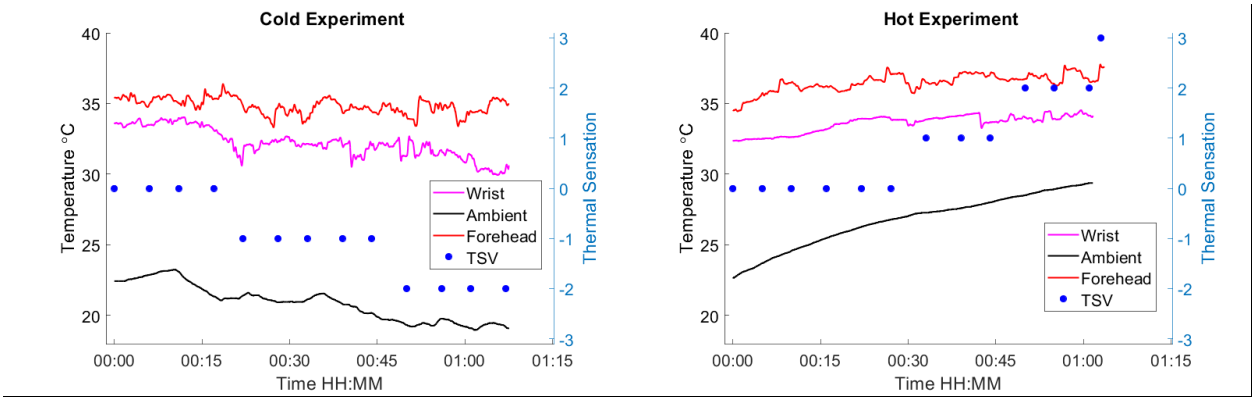

Figure 5: Changes in sensor measurements and corresponding thermal sensation votes of a participant

3.2.3 Model Training and Evaluation

The ASHRAE 7-point thermal sensation scale is the most widely used scale to collect thermal sensations and thus was used in this study to collect thermal sensations. Previous studies have shown that neutral vote of 0 does not necessarily correspond to the desired sensation, and thermal acceptability spans a wider range of thermal sensations than neutral alone [54,55]. Since the primary goal of thermal comfort models is to distinguish between comfortable and uncomfortable states, the ASHRAE 7-point scale was grouped into three categories: Cold (TSV ϵ {-3, -2}), Comfortable (TSV ϵ {-1, 0, +1}) and Hot (TSV ϵ {+2, +3}). This grouping corresponds to the assumption in ASHRAE 55 that occupants are satisfied in the range of $-1.5 \leq TSV \leq +1.5$ when the scale resolution is 0.5 or less, or $-2 < TSV < +2$ when the scale resolution is limited to integers [2]. The thermal satisfaction scale was grouped into two categories: Satisfied (Satisfaction ϵ {0, +1, +2, +3}) and Dissatisfied (Satisfaction ϵ {-1, -2, -3}). ASHRAE 55 suggests this grouping for determining acceptability of the thermal environment, although a slightly broader view of acceptability by including satisfaction vote of -1 as acceptable is also permitted [2]. Furthermore, the thermal sensation and satisfaction votes were combined to create categories that reflect both thermal sensation and satisfaction. For each type of thermal comfort feedback, several ML algorithms were trained and evaluated for each participant. Overall, three different types of models were evaluated separately: 1) Comfort prediction models (cold, comfortable or hot), 2) Satisfaction prediction models (satisfied or dissatisfied) and 3) Combined Comfort and Satisfaction prediction models (cold and satisfied, cold and dissatisfied, comfortable and satisfied, comfortable and dissatisfied, hot and satisfied, or hot and dissatisfied).

In order to compare the performance of different ML algorithms for thermal comfort prediction, we trained several algorithms to build individual comfort models. We evaluated Random Forest, Support Vector Machine (SVM) with quadratic kernel, K-Nearest Neighbor (KNN) with k=1, Subspace KNN, and Subspace Linear Discriminant classification algorithms using a 5-fold cross validation for each participant. In a k fold cross validation, the dataset is randomly partitioned into k subsets and k-1 subsets are used for

training the model and 1 subset is used for model validation and the process is repeated k times. The advantage of using a k fold cross validation is that it generally leads to a more generalizable model and reduces the chances of overfitting the model on the training data. Random Forest, KNN, and SVM methods have been used for thermal comfort prediction in previous studies [11,26,40,41]. Although previous studies have also investigated regression models [42,43], we limit our investigation to classification models because they are more applicable to smaller datasets and are more commonly used in previous studies [11,16,20,26,40,41,44].

The SVM method evaluates an optimal hyperplane in the feature space that separates different classes and using a nonlinear kernel such as a quadratic kernel enables the calculation of the separation hyperplane in a higher dimension, which is capable of creating nonlinear separation boundaries in the feature space. The KNN algorithm assigns the classification label that is most common among its k-nearest neighbors for a data point. The other three methods belong to a class of ensemble methods, which combine multiple weak learners to provide a more robust prediction. The Subspace Discriminant method randomly selects multiple subsets of available features and evaluates a linear discriminant for each subset (weak learner) and combines the predictions from each of the weak learner to output the overall prediction. Similar to Subspace Discriminant, the Subspace KNN method randomly selects multiple subsets to train a weak KNN learner and combines their predictions to output the overall prediction. Random Forest method trains multiple decision trees on random subset of features and combines the output of the decision trees to provide a more robust prediction. The detailed description of the classification algorithms is beyond the scope of this paper and readers are referred to different ML textbooks for further information [56,57].

After selecting important features among the extracted features from section 3.2.2, each of the algorithms mentioned above were used to train individual comfort models using a 5-fold cross validation. In other words, data from each participant was used to train and evaluate the model for the same participant. Because the goal of the study was to evaluate the accuracies of individual comfort models built from different sensing methods, the process of training the models was repeated using features from one sensor at a time and then using features from a combination of different sensors. The accuracy of the models for each participant was obtained from the 5-fold cross validation for each algorithm and each type of sensor. The accuracies were grouped by the algorithms and the sensors used; the average and standard deviation of the accuracy observed among the 20 participants for each algorithm and sensor is reported in section 4.

4 Results

Since the main objective of this study is to evaluate the effectiveness of different sensing methods for individual thermal comfort prediction, we trained the classification algorithms described in section 3.2.3 using the features extracted from a single data stream and with combinations of multiple data streams. The first model predicted thermal sensations. For predicting thermal sensations, TSVs, grouped into cold, comfortable and hot, were used as the labels. The features extracted from different sensors were used as input to the models. Table 2 shows the average and standard deviation of the prediction accuracy for the individual models built by each algorithm for predicting thermal comfort sensations. We observe that the performance of all the classification algorithms are quite similar. SVM with quadratic kernel resulted in a slightly better performance compared to the other evaluated algorithms when looking at the overall average accuracy and standard deviation of the models. Regardless of the classification algorithm used, we see that using ambient temperature alone leads to a higher accuracy (about 81%) compared to using wrist temperature from the wearable device (about 76%) or face temperatures from the thermal camera (about 75%). When the data from wrist or from thermal camera is combined with data from the ambient temperature sensor, prediction accuracy improves to about 83%, and when data from all the sensors are used together, accuracy improves to about 85%.

Table 2: Prediction accuracies for hot, comfortable and cold sensations

Sensor Data used	Subspace KNN	Random Forest	Subspace Discriminant	KNN	Quadratic SVM
Air temperature only	0.79 ± 0.19	0.79 ± 0.19	0.79 ± 0.10	0.80 ± 0.17	0.81 ± 0.15
Wrist temperature only	0.74 ± 0.18	0.76 ± 0.16	0.72 ± 0.17	0.75 ± 0.18	0.76 ± 0.16
Thermal camera only	0.76 ± 0.17	0.76 ± 0.14	0.73 ± 0.11	0.76 ± 0.16	0.75 ± 0.12
Wrist and Air temperature	0.82 ± 0.18	0.81 ± 0.19	0.83 ± 0.09	0.82 ± 0.18	0.83 ± 0.17
Thermal camera and Air temperature	0.79 ± 0.20	0.84 ± 0.16	0.84 ± 0.09	0.85 ± 0.10	0.84 ± 0.15
All Sensors	0.83 ± 0.18	0.84 ± 0.19	0.83 ± 0.10	0.85 ± 0.17	0.85 ± 0.14

Although occupant satisfaction can be approximated from the TSVs using the assumption that occupants are satisfied if -2< TSV<+2, actual satisfaction may be different. In this study, we also collected satisfaction votes from participants using a 7-point satisfaction scale and grouped them into two categories: Satisfied and Dissatisfied as explained in section 3.2.3. We observed that for most of the votes (approx. 81%) align with the assumption that Cold (TSV ≤ -2) and Hot (TSV ≥ +2) result in dissatisfaction and Neutral or Comfortable sensation (-2 < TSV < +2) results in satisfaction. However, a significant portion of the votes (approx. 19%) did not align with the assumption. We observed that sometimes participants are satisfied under cold or hot sensations or dissatisfied under neutral sensations.

To overcome the misalignment between thermal sensation and thermal satisfaction, it might be useful to directly predict thermal satisfaction instead of predicting thermal sensations. Therefore, the second model predicted thermal satisfaction. We repeated the same model training and evaluation process described in section 3.2.3, replacing thermal sensations with thermal satisfaction in order to directly predict thermal satisfaction. For predicting thermal satisfaction, satisfaction votes, which were grouped into satisfied and dissatisfied, were used as the labels. The features extracted from different sensors were used as input to the models. Table 3 shows the accuracies of different sensing methods and algorithms to predict satisfied and dissatisfied conditions. We observe that all the algorithms perform well with accuracies in the range of 85% to 94% with KNN performing slightly better than other algorithms in terms of accuracy. It is important to note that since we are only predicting two classes of satisfaction, the accuracies are higher than predicting 3 classes of thermal sensation. Regardless of the algorithm used, we observe that using data from the ambient sensor results in a slightly better accuracy compared to using data from wearable device or thermal camera only. Accuracy improves slightly when data from the ambient sensor is added to data from the wearable device or from the thermal camera.

Table 3 : Prediction accuracies for satisfied and dissatisfied thermal conditions

Sensor Data used	Subspace KNN	Random Forest	Subspace Discriminant	KNN	Quadratic SVM
Air temperature only	0.92 ± 0.08	0.92 ± 0.08	0.89 ± 0.10	0.93 ± 0.08	0.92 ± 0.07
Wrist temperature only	0.87 ± 0.11	0.88 ± 0.11	0.85 ± 0.12	0.87 ± 0.12	0.88 ± 0.11
Thermal camera only	0.89 ± 0.10	0.87 ± 0.10	0.87 ± 0.10	0.89 ± 0.10	0.85 ± 0.11
Wrist and Air temperature	0.94 ± 0.07	0.94 ± 0.06	0.89 ± 0.08	0.94 ± 0.07	0.93 ± 0.07
Thermal camera and Air temperature	0.91 ± 0.10	0.92 ± 0.09	0.89 ± 0.08	0.92 ± 0.11	0.92 ± 0.07
All Sensors	0.92 ± 0.08	0.94 ± 0.06	0.91 ± 0.07	0.94 ± 0.07	0.93 ± 0.06

For controlling the thermal environment, knowing whether the occupant is satisfied or dissatisfied is not sufficient because the dissatisfaction might result from hot or cold sensation. The third model predicts thermal sensation and satisfaction.. The thermal sensation includes three classes: cold, comfortable or hot, and thermal satisfaction includes two classes: satisfied or dissatisfied. The combined comfort and satisfaction include six classes obtained by creating a class for each possible combination of thermal sensation and satisfaction, namely: cold and satisfied, cold and dissatisfied, comfortable and satisfied, comfortable and dissatisfied, hot and satisfied, or hot and dissatisfied. For predicting combined thermal sensations and satisfaction, the six classes obtained by combining thermal sensation and satisfaction were used as the labels. The features extracted from different sensors were used as input to the models. We repeated the model training and evaluation as described in section 3.2.3Table 4 shows the results of combined prediction of thermal sensation and satisfaction. Since there are six classes to classify, the prediction accuracy is lower than the accuracy of predicting the thermal sensation or satisfaction, separately. Regardless of the classification algorithm used, we observe that using data from the ambient temperature sensor alone results in a higher accuracy than using data from the wearable device or the thermal camera alone. Similar to previous models, the prediction accuracy improves slightly when information from the ambient temperature sensor is combined with other sensors.

Table 4: Accuracies for combined thermal sensation and satisfaction prediction

Sensor Data used	Subspace KNN	Random Forest	Subspace Discriminant	KNN	Quadratic SVM
Air temperature only	0.70 ± 0.19	0.72 ± 0.21	0.72 ± 0.11	0.71 ± 0.21	0.72 ± 0.14
Wrist temperature only	0.63 ± 0.20	0.66 ± 0.19	0.62 ± 0.16	0.64 ± 0.21	0.67 ± 0.17
Thermal camera only	0.67 ± 0.20	0.68 ± 0.19	0.65 ± 0.13	0.68 ± 0.19	0.68 ± 0.16
Wrist and Air temperature	0.72 ± 0.22	0.75 ± 0.20	0.72 ± 0.12	0.74 ± 0.21	0.75 ± 0.15
Thermal camera and Air temperature	0.75 ± 0.23	0.72 ± 0.20	0.74 ± 0.11	0.75 ± 0.21	0.75 ± 0.16
All Sensors	0.74 ± 0.22	0.73 ± 0.22	0.73 ± 0.12	0.76 ± 0.22	0.75 ± 0.17

The feature selection using Neighborhood Components described in section 3.2.3 evaluates the weight of each feature based on its importance for the classification problem. We also ranked the most important features for each type of classification problem based on their feature weights. Table 5 lists 10 most important features for predicting thermal sensation, thermal satisfaction or combined sensation and satisfaction. We observe that features related to the ambient temperature are ranked higher in the list compared to other sensing methods. We also observe that most of the important features relate to the most recent measurements (last point and average of last 10 seconds), direct value of the measurements (min, max, average, median etc.), and some features relate to the shape of the data stream (linB and quadC which are coefficients of first and second order polynomials). Features related to the gradient of data stream were relatively less important based on their feature weights. This finding aligns with [11] where gradient based features were not found very useful for predicting thermal sensations. We also observe that among the studied locations in the face, nose seems to be more important compared to other locations.

Table 5: Ten most important features for each type of classification problem when using all sensors

Thermal Sensation prediction	Thermal Satisfaction prediction	Combined Sensation and Satisfaction prediction

AmbTemp_lastPoint	AmbTemp_lastPoint	AmbTemp_lastPoint
AmbTemp_min	AmbTemp_quadC	AmbTemp_max
AmbTemp_max	AmbTemp_last10Avg	AmbTemp_avg
AmbTemp_avg	WristTemp_last10Avg	AmbTemp_min
AmbTemp_quadC	AmbTemp_min	AmbTemp_last10Avg
AmbTempr_last10Avg	AmbTemp_max	AmbTemp_median
NoseTemp_last10Avg	AmbTemp_linB	AmbTemp_linB
WristTemp_last10Avg	NoseTemp_linB	AmbTemp_quadC
AmbTemp_linB	NoseTemp_last10Avg	WristTemp_median
Rcheek_min	NoseTemp_lastPoint	WristTemp_lastPoint

Note: linB and quadC refer to the coefficients of best-fit polynomials of the form $y = Ax + B$ (linear) and $y = Ax^2 + Bx + C$ (quadratic) which capture the shape of the data stream.

5 Discussion

One of the interesting observations of this study is that all of the selected algorithms performed similarly. Among the studied algorithms, SVM with quadratic kernel performed slightly better than other algorithms. These algorithms were selected based on their utilization by the prior studies [11,26,40,41] and on their performance in similar classification problems, so a high accuracy was expected from the algorithms. Another reason for similar performance is that a feature selection was performed prior to training the models, which resulted in only useful features being used for training the models.

Interestingly, the general trend was that the data from the ambient temperature sensor alone led to a higher accuracy for both thermal sensation and satisfaction prediction compared to the physiological data alone, regardless of the algorithm used for training the models. Furthermore, the features extracted from the ambient temperature sensor were ranked higher than the features from other sensors as shown in Table 5. Although the results seem a bit counterintuitive because ambient temperature was a better predictor of thermal sensation compared to the skin temperature, it is supported by the prediction accuracies shown in Tables 2-4 and ranking of features shown in Table 5. One of the potential reasons for lower accuracy from wearable devices or thermal cameras is that these devices are prone to high levels of noise in the data. Another reason is that the changes in skin temperatures are much smaller compared to the changes in ambient temperature. Since ambient temperature was the only factor changed during the experiment, and there were no other heat sources such as solar radiation or local comfort devices, changes in ambient temperature was a better predictor of thermal comfort. As seen from Figure 3 and Figure 5, there are several places where there is a sudden change in the sensor measurements of the wearable device as well as the thermal camera. Sudden movement of the wrist worn device or sudden movement of the face relative to the thermal camera can lead to a nosier signal. Ambient sensors are less prone to sudden variations in sensor measurement and thus have less noise in the sensor signals. Furthermore, the low accuracy of thermal camera, ±5 °C compared to ±0.5 °C accuracy of other sensors means that the thermal camera may not be able to monitor minor changes in skin temperature, which could have resulted in a lower accuracy of thermal comfort prediction using the thermal camera. Additional information, such as clothing surface temperature, obtained from the thermal camera [58,59] could potentially improve the accuracy of the models built using thermal camera. However, it was not possible to automatically extract clothing surface temperatures in our study because very little clothing was visible in the thermal images captured during this study. Future studies can investigate adding clothing related information from thermal images to improve the accuracy of individual comfort models.

Our results indicate that combining both physiological data and environmental data improves the model accuracy compared to using environmental data alone. However, under the conditions studied, the improvement in accuracy from using physiological data is fairly small (about 3% to 4%) compared to using environmental data alone. From a practical perspective, the slight improvement in accuracy might not be enough to justify the additional cost of deploying wearable devices or thermal cameras to monitor and predict thermal comfort. The cost of FLIR Lepton is about $250; it is on the cheaper end of thermal cameras currently available in the market. Smartwatches with skin temperature sensor cost upwards of $100, whereas ambient air temperature sensors cost upwards of $5. Wearable devices or thermal cameras could raise privacy concerns among occupants, whereas ambient sensors are less prone to privacy concerns. In cases where occupants might already wear smartwatches that monitor skin temperature and are willing to provide access to the data, using the data from those devices to improve thermal comfort prediction might be useful.

The study involved 20 participants with different ages and body composition as shown in Table 1. Since the goal of this study was to compare the accuracies of individual comfort models, having a wide range of age and body composition is beneficial towards the goal of the study because it enabled us to evaluate the models for participants of different age and body compositions. Although differences in thermal sensations exist between different genders, gender was not explicitly considered because separate models were built for each participant. The feature extraction process resulted in a total of 543 sets of features and corresponding TSVs, which is equivalent to roughly 27 TSVs per participant. The prediction accuracies of approximately 85% for thermal sensation, which was obtained in this study is comparable to previous studies that used ambient temperature combined with wrist temperatures, 87% in [40], or facial temperatures, 83% in [16] and 85% in [11]. The higher accuracy of about 93% observed when predicting thermal satisfaction results from the fact that it is classifying two classes (satisfied vs dissatisfied). Similar accuracy of around 95% was observed in a previous study when predicting comfortable vs uncomfortable sensations when separate models for heating (comfortable vs hot) and cooling (comfortable vs cold) conditions were used [44].

The range of temperatures investigated in this study are wider than what is typically found in actual offices, and the temperature was rapidly changed in a relatively short duration which is not common in actual offices. Long term studies in stable environments are needed to confirm the findings of this study in real offices. Another limitation of this study is that the experiments were conducted during the summer season in Los Angeles and the participants wore summer clothing (t-shirt and pants). The results might also differ in different seasons and clothing insulations. Furthermore, the comfort ranges of people from Los Angeles might be different from people in other locations due to thermal acclimatization. Future studies are necessary to investigate the tradeoffs of using different sensing methods under different seasons, climates and different clothing insulations.

The conditions investigated in this study are specific and broad generalizations cannot be made without further investigation. The experiment was conducted in a room without a window (i.e. no radiant heat from the sun) and the only parameter changed in the study was the air temperature. The conditions studied are similar to what can be found in offices that are not along the building perimeter, or where shading devices block the direct radiation from the sun. Therefore, the results might not hold for situations where radiant heat sources or local comfort devices are present. Further studies are necessary to investigate the tradeoffs of using physiological sensing to improve thermal comfort models under different environmental conditions where radiant heat sources or local comfort devices are present.

The dataset in this study is comparable to previous studies in terms of number of participants, and number of TSVs collected [11,15,19,40,41,60,61]. The study duration and methodology to explore a wide range of

temperatures in a relatively short duration is also comparable to previous studies [11,15,19,40,41,60,61]. However, even though the dataset is comparable to previous studies, neither the present study nor the prior studies in the literature are large enough or long enough to draw broadly generalizable conclusions. Currently available global comfort databases were created by collaborations at a global scale and contain data regarding environmental parameters and occupant feedback [62,63]. However, unfortunately, the existing databases do not contain physiological measurements. A similar concerted effort from a large group of researchers is needed to create a global dataset with physiological changes under different environmental conditions to draw generalizable conclusions that will apply under various conditions.

6 Conclusion

Current methods of evaluating thermal comfort in buildings are unable to accommodate individual differences in thermal sensations and preferences due to their "one size fits all" approach. In order to overcome the limitations of existing methods, there has been an increasing interest in modeling and predicting thermal comfort at an individual level to improve the controls of HVAC systems or other local comfort systems. Individual comfort models typically rely on the data from environmental and/or physiological sensors and leverage different ML algorithms to predict thermal comfort sensations. Recently, several studies have utilized data from wearable devices or thermal cameras to monitor skin temperature from the wrist or facial region for predicting thermal comfort. These previous studies relied on different sensing methods and different algorithms for modeling thermal comfort, which made it difficult to directly compare the effectiveness of different sensing and modeling methods. In this study, we presented a direct comparison of modeling and predicting thermal sensations and thermal satisfaction using different sensing and modeling methods. We compared ambient air temperature, wrist skin temperature from a wearable device and facial skin temperature from a thermal camera as different sensing methods using five different ML algorithms for modeling thermal comfort at an individual level.

Our results indicate that using information from the environmental sensor results in a higher accuracy compared to using physiological information from the wearable device or the thermal camera only. Combining data from the environmental sensor with data from the physiological sensor results in 3% to 5% improvement in prediction of thermal sensation when compared to using data from environmental sensor only. The prediction accuracies of different ML algorithms evaluated in this study were quite similar and the trend of environmental data being more useful than physiological data was consistent among the studied algorithms. The results are also supported by the relative importance of features ranked using Neighborhood Components Analysis, where features from the environmental sensor were ranked higher than features from other sensors. The small improvement of 3% to 5% in prediction accuracy might not be sufficient to justify the additional cost and potential privacy concerns of using physiological data for predicting thermal comfort. The results may be applicable to environments, which do not have any direct radiant heat sources or local comfort devices, such as rooms that are not along the building perimeter.

The study involved a controlled experiment with 20 participants where air temperature was gradually changed, and no other heat sources or local comfort devices were present. More comprehensive studies are necessary to confirm the findings of this study and to investigate the other conditions such as different seasons and climate types. Future studies are necessary to compare the effectiveness of different sensing methods for predicting thermal comfort in environments with radiant heat sources or local comfort devices. The results of this study suggest that in some conditions, monitoring environmental parameters might be more useful and practical for predicting thermal comfort compared to monitoring physiological parameters. It is therefore important to understand the tradeoffs of using different sensing methods under different conditions if different sensors are to be deployed at large scales. There is a potential to reduce deployment costs and avoid privacy issues when only environmental parameters are monitored.

Acknowledgements

This material is based upon the work supported by the National Science Foundation under Grant No. 1763134 and 1351701. Any opinions, findings, and conclusions or recommendations expressed in this material are those of the authors and do not necessarily reflect the views of the National Science Foundation. The help of research assistants Paulina Maldonado, Eddy Solares Quezada, Irie Cooper and Victoria Sanchez is greatly appreciated.

References

[1] C. Karmann, S. Schiavon, E. Arens, Percentage of commercial buildings showing at least 80% occupant satisfied with their thermal comfort, Proc. 10th Wind. Conf. Rethink. Comf. (2018). https://cloudfront.escholarship.org/dist/prd/content/qt89m0z34x/qt89m0z34x.pdf?t=p9m07w.

[2] ASHRAE, ASHRAE Standard 55-2017:"Thermal Environmental Conditions for Human Occupancy," (2017). https://www.ashrae.org/technical-resources/standards-and-guidelines/read-only-versions-of-ashrae-standards.

[3] S. International Standard Organization, Geneva, ISO 7730:2005(en), Ergonomics of the thermal environment — Analytical determination and interpretation of thermal comfort using calculation of the PMV and PPD indices and local thermal comfort criteria, 2005. https://www.iso.org/obp/ui/#iso:std:iso:7730:ed-3:v1:en.

[4] L. Pérez-Lombard, J. Ortiz, C. Pout, A review on buildings energy consumption information, Energy Build. 40 (2008) 394–398. doi:10.1016/j.enbuild.2007.03.007.

[5] A. Aryal, B. Becerik-Gerber, Energy consequences of Comfort-driven temperature setpoints in office buildings, Energy Build. 177 (2018) 33–46. doi:10.1016/j.enbuild.2018.08.013.

[6] T. Cheung, S. Schiavon, T. Parkinson, P. Li, G. Brager, Analysis of the accuracy on PMV – PPD model using the ASHRAE Global Thermal Comfort Database II, Build. Environ. (2019). doi:10.1016/J.BUILDENV.2019.01.055.

[7] J. Kim, S. Schiavon, G. Brager, Personal comfort models – A new paradigm in thermal comfort for occupant-centric environmental control, Build. Environ. 132 (2018) 114–124. doi:10.1016/j.buildenv.2018.01.023.

[8] D. Daum, F. Haldi, N. Morel, A personalized measure of thermal comfort for building controls, Build. Environ. 46 (2011) 3–11. doi:10.1016/j.buildenv.2010.06.011.

[9] A. Ghahramani, C. Tang, B. Becerik-gerber, An online learning approach for quantifying personalized thermal comfort via adaptive stochastic modeling, Build. Environ. 92 (2015) 86–96. doi:10.1016/j.buildenv.2015.04.017.

[10] F. Jazizadeh, A. Ghahramani, B. Becerik-Gerber, T. Kichkaylo, M. Orosz, Personalized Thermal Comfort-Driven Control in HVAC-Operated Office Buildings, in: ASCE Int. Work. Comput. Civ. Eng., American Society of Civil Engineers, Reston, VA, 2013: pp. 218–225. http://ascelibrary.org/doi/abs/10.1061/9780784413029.028.

[11] D. Li, C.C. Menassa, V.R. Kamat, Non-Intrusive Interpretation of Human Thermal Comfort through Analysis of Facial Infrared Thermography, Energy Build. (2018). doi:10.1016/J.ENBUILD.2018.07.025.

[12] S. Lee, P. Karava, A. Tzempelikos, I. Bilionis, Inference of thermal preference profiles for personalized thermal environments with actual building occupants, Build. Environ. 148 (2019) 714–729. doi:10.1016/J.BUILDENV.2018.10.027.

[13] J.-H. Choi, D. Yeom, Development of the data-driven thermal satisfaction prediction model as a function of human physiological responses in a built environment, Build. Environ. 150 (2019) 206–218. doi:10.1016/J.BUILDENV.2019.01.007.

[14] J. Xiong, X. Zhou, Z. Lian, J. You, Y. Lin, Thermal perception and skin temperature in different transient thermal environments in summer, Energy Build. 128 (2016) 155–163. doi:10.1016/j.enbuild.2016.06.085.

[15] J.-H. Choi, D. Yeom, Study of data-driven thermal sensation prediction model as a function of local body skin temperatures in a built environment, Build. Environ. 121 (2017) 130–147. doi:10.1016/j.buildenv.2017.05.004.

[16] A. Ghahramani, G. Castro, S.A. Karvigh, B. Becerik-Gerber, Towards unsupervised learning of thermal comfort using infrared thermography, Appl. Energy. 211 (2018) 41–49. doi:10.1016/J.APENERGY.2017.11.021.

[17] S. Liu, M. Jin, H.P. Das, C.J. Spanos, S. Schiavon, Personal thermal comfort models based on physiological parameters measured by wearable sensors, in: Proc. Wind. Conf., 2018: pp. 431–441.

[18] B. Pavlin, G. Pernigotto, F. Cappelletti, P. Bison, R. Vidoni, A. Gasparella, B. Pavlin, G. Pernigotto, F. Cappelletti, P. Bison, R. Vidoni, A. Gasparella, Real-Time Monitoring of Occupants' Thermal Comfort through Infrared Imaging: A Preliminary Study, Buildings. 7 (2017) 10. doi:10.3390/buildings7010010.

[19] A.C. Cosma, R. Simha, Thermal comfort modeling in transient conditions using real-time local body temperature extraction with a thermographic camera, Build. Environ. 143 (2018) 36–47. doi:10.1016/J.BUILDENV.2018.06.052.

[20] M. Burzo, C. Wicaksono, M. Abouelenien, V. Perez-Rosas, R. Mihalcea, Y. Tao, Multimodal sensing of thermal discomfort for adaptive energy saving in buildings, IiSBE NET ZERO BUILT Environ. (2014) 344.

[21] P.O. Fanger, Analysis and Applications in Environmental Engineering, Danish Tech. Press. (1970) 244. https://www.cabdirect.org/cabdirect/abstract/19722700268 (accessed January 23, 2018).

[22] R.J. De Dear, G.S. Brager, Developing an adaptive model of thermal comfort and preference, ASHRAE Trans. 104 (1998) 145. https://escholarship.org/uc/item/4qq2p9c6.

[23] J. van Hoof, Forty years of Fanger's model of thermal comfort: comfort for all?, Indoor Air. 18 (2008) 182–201. doi:10.1111/j.1600-0668.2007.00516.x.

[24] R.J. De Dear, T. Akimoto, E.A. Arens, G. Brager, C. Candido, K.W.D. Cheong, B. Li, N. Nishihara, S.C. Sekhar, S. Tanabe, J. Toftum, H. Zhang, Y. Zhu, Progress in thermal comfort research over the last twenty years, Indoor Air. 23 (2013) 442–461. doi:10.1111/ina.12046.

[25] J.F. Nicol, M.A. Humphreys, Adaptive thermal comfort and sustainable thermal standards for buildings, Energy Build. 34 (2002) 563–572. doi:10.1016/S0378-7788(02)00006-3.

[26] M. Feldmeier, J.A. Paradiso, Personalized HVAC control system, in: 2010 Internet Things, IEEE, 2010: pp. 1–8. doi:10.1109/IOT.2010.5678444.

[27] Q. Zhao, Y. Zhao, F. Wang, J. Wang, Y. Jiang, F. Zhang, A data-driven method to describe the personalized dynamic thermal comfort in ordinary office environment: From model to application, Build. Environ. 72 (2014) 309–318. doi:10.1016/j.buildenv.2013.11.008.

[28] F. Jazizadeh, A. Ghahramani, B. Becerik-Gerber, T. Kichkaylo, M. Orosz, Human-Building

Interaction Framework for Personalized Thermal Comfort-Driven Systems in Office Buildings, J. Comput. Civ. Eng. 28 (2014) 2–16. doi:10.1061/(ASCE)CP.1943-5487.0000300.

[29] L. Jiang, R. Yao, Modelling personal thermal sensations using C-Support Vector Classification (C-SVC) algorithm, Build. Environ. 99 (2016) 98–106. doi:10.1016/J.BUILDENV.2016.01.022.

[30] D. Li, C.C. Menassa, V.R. Kamat, Personalized human comfort in indoor building environments under diverse conditioning modes, Build. Environ. (2017). doi:10.1016/j.buildenv.2017.10.004.

[31] E. Arens, H. Zhang, The skin's role in human thermoregulation and comfort, in: Therm. Moisture Transp. Fibrous Mater., 2006: pp. 560–602. doi:10.1533/9781845692261.3.560.

[32] H. Zhang, E. Arens, C. Huizenga, T. Han, Thermal sensation and comfort models for non-uniform and transient environments, part III: Whole-body sensation and comfort, Build. Environ. 45 (2010) 399–410. doi:10.1016/j.buildenv.2009.06.020.

[33] H. Zhang, E. Arens, C. Huizenga, T. Han, Thermal sensation and comfort models for non-uniform and transient environments: Part I: Local sensation of individual body parts, Build. Environ. 45 (2010) 380–388. doi:10.1016/j.buildenv.2009.06.018.

[34] E. Arens, H. Zhang, C. Huizenga, Partial- and whole-body thermal sensation and comfort— Part I: Uniform environmental conditions, J. Therm. Biol. 31 (2006) 53–59. doi:10.1016/J.JTHERBIO.2005.11.028.

[35] E. Arens, H. Zhang, C. Huizenga, Partial- and whole-body thermal sensation and comfort—Part II: Non-uniform environmental conditions, J. Therm. Biol. 31 (2006) 60–66. doi:10.1016/J.JTHERBIO.2005.11.027.

[36] H. Zhang, E. Arens, C. Huizenga, T. Han, Thermal sensation and comfort models for non-uniform and transient environments, part II: Local comfort of individual body parts, Build. Environ. 45 (2010) 389–398. doi:10.1016/j.buildenv.2009.06.015.

[37] H. Zhang, Human thermal sensation and comfort in transient and non-uniform thermal environments, 2008. https://escholarship.org/uc/item/11m0n1wt (accessed February 8, 2019).

[38] Y. Yao, Z. Lian, W. Liu, Q. Shen, Experimental study on physiological responses and thermal comfort under various ambient temperatures, Physiol. Behav. 93 (2008) 310–321. doi:10.1016/J.PHYSBEH.2007.09.012.

[39] T. Sakoi, K. Tsuzuki, S. Kato, R. Ooka, D. Song, S. Zhu, Thermal comfort, skin temperature distribution, and sensible heat loss distribution in the sitting posture in various asymmetric radiant fields, Build. Environ. 42 (2007) 3984–3999. doi:10.1016/J.BUILDENV.2006.10.050.

[40] T. Chaudhuri, D. Zhai, Y.C. Soh, H. Li, L. Xie, Thermal comfort prediction using normalized skin temperature in a uniform built environment, Energy Build. 159 (2018) 426–440. doi:10.1016/j.enbuild.2017.10.098.

[41] T. Chaudhuri, D. Zhai, Y.C. Soh, H. Li, L. Xie, Random forest based thermal comfort prediction from gender-specific physiological parameters using wearable sensing technology, Energy Build. 166 (2018) 391–406. doi:10.1016/J.ENBUILD.2018.02.035.

[42] S.Y. Sim, M.J. Koh, K.M. Joo, S. Noh, S. Park, Y.H. Kim, K.S. Park, Estimation of thermal sensation based on wrist skin temperatures, Sensors (Switzerland). 16 (2016) 420. doi:10.3390/s16040420.

[43] M. Abdallah, C. Clevenger, T. Vu, A. Nguyen, Sensing Occupant Comfort Using Wearable

Technologies, in: Constr. Res. Congr. 2016, American Society of Civil Engineers, Reston, VA, 2016: pp. 940–950. doi:10.1061/9780784479827.095.

[44] J. Ranjan, J. Scott, ThermalSense, in: Proc. 2016 ACM Int. Jt. Conf. Pervasive Ubiquitous Comput. - UbiComp '16, ACM Press, New York, New York, USA, 2016: pp. 1212–1222. doi:10.1145/2971648.2971659.

[45] J.-H.H. Choi, V. Loftness, D.-W.W. Lee, Investigation of the possibility of the use of heart rate as a human factor for thermal sensation models, Build. Environ. 50 (2012) 165–175. doi:10.1016/j.buildenv.2011.10.009.

[46] W. Liu, Z. Lian, Y. Liu, Heart rate variability at different thermal comfort levels, Eur. J. Appl. Physiol. 103 (2008) 361–366. doi:10.1007/s00421-008-0718-6.

[47] M.C. Peel, B.L. Finlayson, T.A. McMahon, Updated world map of the Köppen-Geiger climate classification, Hydrol. Earth Syst. Sci. 11 (2007) 1633–1644. doi:10.5194/hess-11-1633-2007.

[48] FLIR, FLIR LEPTON® with Radiometry Datasheet, 2016. www.flir.com/globalassets/imported-assets/document/lepton-engineering-datasheet---with-radiometry.pdf.

[49] I. Ben-Gal, Outlier detection, in: Data Min. Knowl. Discov. Handb., Springer, 2005: pp. 131–146.

[50] R.W. Schafer, What is a Savitzky-Golay filter, IEEE Signal Process. Mag. 28 (2011) 111–117.

[51] H. Metzmacher, D. Wölki, C. Schmidt, J. Frisch, C. van Treeck, Real-time human skin temperature analysis using thermal image recognition for thermal comfort assessment, Energy Build. 158 (2018) 1063–1078. doi:10.1016/J.ENBUILD.2017.09.032.

[52] V. Kazemi, J. Sullivan, One millisecond face alignment with an ensemble of regression trees, in: 2014 IEEE Conf. Comput. Vis. Pattern Recognit., IEEE, 2014: pp. 1867–1874. doi:10.1109/CVPR.2014.241.

[53] W. Yang, K. Wang, W. Zuo, Neighborhood Component Feature Selection for High-Dimensional Data, J. Comput. 7 (2012). doi:10.4304/jcp.7.1.161-168.

[54] F.S.B. Brager, G.S., M.E. Fountain, C.C. Benton, E.A. Arens, A Comparison of Methods for Assessing Thermal Sensation and Acceptability in the Field, Proc. Conf. Therm. Comf. Past, Present Futur. Wat- Ford, U.K Build. Res. Establ. (1993) 17–39. doi:10.1080/09613218.2011.556008.

[55] M.A. Humphreys, M. Hancock, Do people like to feel 'neutral'?: Exploring the variation of the desired thermal sensation on the ASHRAE scale, Energy Build. 39 (2007) 867–874. doi:10.1016/J.ENBUILD.2007.02.014.

[56] G. James, D. Witten, T. Hastie, R. Tibshirani, An Introduction to Statistical Learning, Springer New York, New York, NY, 2013. doi:10.1007/978-1-4614-7138-7.

[57] E. Alpaydin, Introduction to machine learning, MIT press, 2014.

[58] R.A. Angelova, E. Georgieva, D. Markov, T. Bozhkov, I. Simova, N. Kehaiova, P. Stankov, Estimating the Effect of Torso Clothing Insulation on Body Skin and Clothing Temperatures in a Cold Environment Using Infrared Thermography, Fibres Text. East. Eur. 26 (2018) 122–129. doi:10.5604/01.3001.0012.1323.

[59] J.-H. Lee, Y.-K. Kim, K.-S. Kim, S. Kim, J.-H. Lee, Y.-K. Kim, K.-S. Kim, S. Kim, Estimating Clothing Thermal Insulation Using an Infrared Camera, Sensors. 16 (2016) 341. doi:10.3390/s16030341.

[60] C. Dai, H. Zhang, E. Arens, Z. Lian, Machine learning approaches to predict thermal demands using skin temperatures: Steady-state conditions, Build. Environ. 114 (2017) 1–10. doi:10.1016/j.buildenv.2016.12.005.

[61] J.-H. Choi, D. Yeom, Investigation of the relationships between thermal sensations of local body areas and the whole body in an indoor built environment, Energy Build. 149 (2017) 204–215. doi:10.1016/j.enbuild.2017.05.062.

[62] R.J. de Dear, A Global Database of Thermal Comfort Field Experiments, ASHRAE Trans. 104 (1998) 1141. https://search.proquest.com/docview/192542601.

[63] V. Földváry Ličina, T. Cheung, H. Zhang, R. de Dear, T. Parkinson, E. Arens, C. Chun, S. Schiavon, M. Luo, G. Brager, P. Li, S. Kaam, M.A. Adebamowo, M.M. Andamon, F. Babich, C. Bouden, H. Bukovianska, C. Candido, B. Cao, S. Carlucci, D.K.W. Cheong, J.-H. Choi, M. Cook, P. Cropper, M. Deuble, S. Heidari, M. Indraganti, Q. Jin, H. Kim, J. Kim, K. Konis, M.K. Singh, A. Kwok, R. Lamberts, D. Loveday, J. Langevin, S. Manu, C. Moosmann, F. Nicol, R. Ooka, N.A. Oseland, L. Pagliano, D. Petráš, R. Rawal, R. Romero, H.B. Rijal, C. Sekhar, M. Schweiker, F. Tartarini, S. Tanabe, K.W. Tham, D. Teli, J. Toftum, L. Toledo, K. Tsuzuki, R. De Vecchi, A. Wagner, Z. Wang, H. Wallbaum, L. Webb, L. Yang, Y. Zhu, Y. Zhai, Y. Zhang, X. Zhou, Development of the ASHRAE Global Thermal Comfort Database II, Build. Environ. 142 (2018) 502–512. doi:10.1016/J.BUILDENV.2018.06.022.